POAC'15
Trondheim, Norway

Proceedings of the 23rd International Conference on
Port and Ocean Engineering under Arctic Conditions
June 14-18, 2015
Trondheim, Norway

MARINE ICING SEVERITY IN THE BARENTS SEA

S. H. Teigen[1], E. S. Hansen[1] and J. C. Roth[2]
[1]Statoil ASA, Bergen, Norway
[2]Statoil ASA, Stavanger, Norway

ABSTRACT

Assessment of the frequency and severity of marine icing of vessels and offshore structures is important as year-round oil and gas operations are gradually moving northwards in the Barents Sea. Utilizing an efficient numerical model for marine icing, estimates of icing severity have been derived for a reference cylindrical geometry, relevant for offshore structures in the area. Input to the model is NORA10 hindcast data of required meteorological parameters from the period 1957 – 2014. The model has been systematically run for grid points covering the Norwegian sector of the southern Barents Sea, enabling to establish contour maps of extreme values for marine icing. Predominant direction of maximum ice build-up and the seasonal variation in icing severity are also investigated.

INTRODUCTION

Some of the most telling images of marine icing are photographs of heavily iced warships during the Second World War. The Allies conducted convoys to the ice free harbours in Russia to support the Soviet Union with military equipment. The convoys were carried out under the danger of airstrikes and submarine attacks, and had to press on regardless of the weather conditions (Edwards, 2002). An inquiry of the loss of the two escort vessels HM Whalers "Shera" and "Sulla" was not conclusive, but pointed out that the vessels had poor stability from the outset due to the amount of extra fuel they had to carry for the long transit, which together with the icing conditions they faced would be a fatal combination (Boards of inquiry and disciplinary courts, 1942). These wartime tragedies and other accidents with fishing and sealing vessels inspired the first efforts to forecast and model marine icing. In general, methods for estimating icing can be divided into two categories, 1) Statistical/empirical relations between key weather parameters and icing rate established by records from fishing vessels (these models are still being used by forecasting agencies) and 2) Theoretically founded models with semi-empirical formulations for e.g. spray flux. In the present study, the three-dimensional, time dependent model described by (Hansen & Teigen, 2015) is utilized for making a basin-wide study of icing conditions in the Barents Sea.

DATA AND METHODS

The input structural geometry considered in the present study is a reference cylindrical structure of 20 m diameter and 20 m height (Figure 1). This is representative for a columnar leg on a semi-submersible drilling rig or production platform. The structure is assumed to be stationary with respect to incoming waves and the other legs of the platform are assumed to

not affect the icing. Using a circular symmetric and relatively simple geometry has some benefits, limiting the number of grid panels needed for resolving the geometry (reducing computational time), but also enabling an analysis of the direction where the worst icing occurs and relate that to prevailing weather conditions. Another advantage is that although spray data is scarce for various vessel and platform types, there is a relatively well documented data set for the spray flux on a semi-submersible (Jørgensen, 1984). The vertical resolution of the grid is refined close to the sea surface to better resolve the effect of icing accumulation being washed away by the waves.

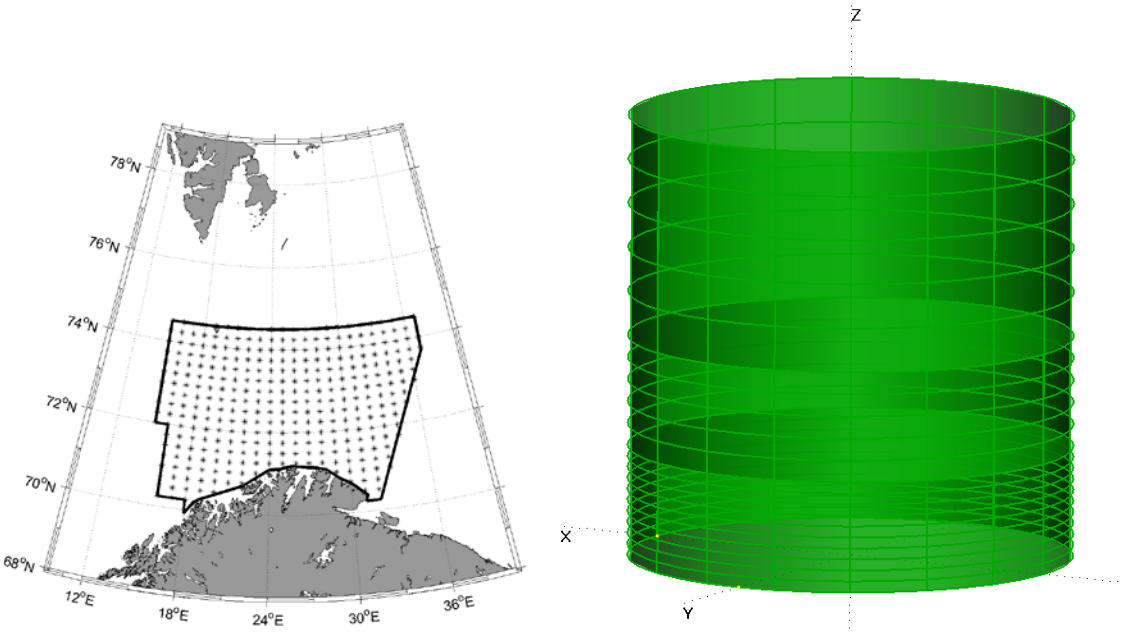

Figure 1 Map showing grid points covering the southern part of the Norwegian Barents Sea (left panel). Reference cylindrical structure used in icing calculations, with numerical grid indicated (right panel).

The analysis is run for the entire NORA10 (Reistad, 2011) hindcast period (1957 – 2014), covering 329 gridpoints in the southern Barents Sea with a time resolution of 3 hours (Figure 1). All time series of environmental parameters (air temperature, humidity, wind speed/direction, wave height/period/direction) that enter the model come from the hindcast archive, except for sea surface temperature. The sea surface temperature is derived from monthly mean values from the World Ocean Atlas (National Oceanographic Data Center, 2013).

The icing rate on every panel on the structure is determined for each 3 hour time segment in the hindcast time series, utilizing the numerical model NuMIS, described in (Hansen & Teigen, 2015). When run in parallel on twelve processors, the analysis for the entire southern Barents Sea takes about 72 hours. The extreme or 100 year values of total accreted ice mass on the cylinder are calculated by fitting the set of yearly extremes to a Gumbel distribution. The statistical method is described in (Hansen, et al., 2015).

RESULTS

Maximum accumulated icing throughout the hindcast period

A contour map of the maximum simulated ice mass on the column at each geographical grid point throughout the hindcast period is plotted in Figure 2. The maximum mass varies from about 60 tons in the southeastern corner (north of Tromsø) to 200 tons north of 74°N. Note that the maximum event could happen in different years from location to location.

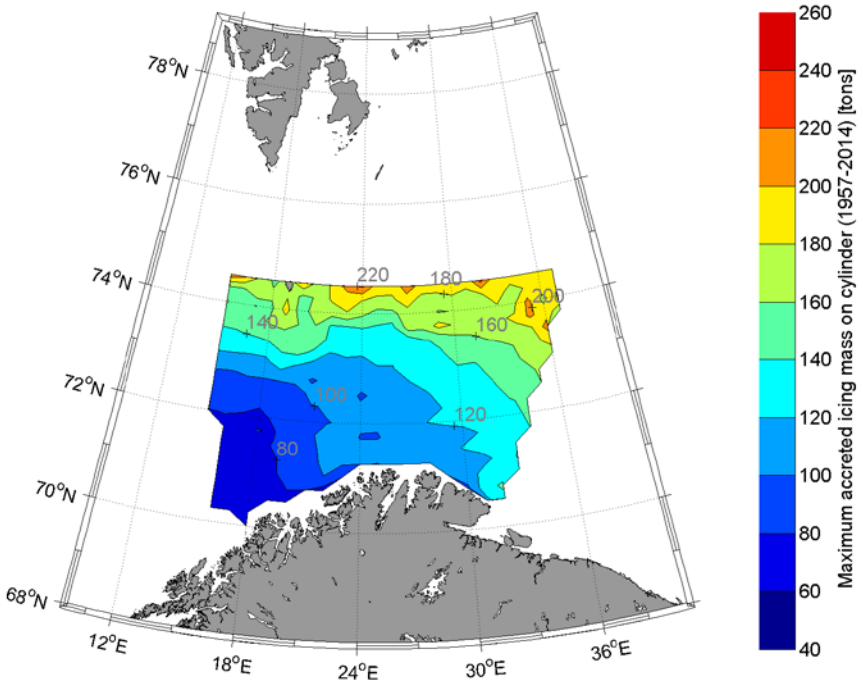

Figure 2 Maximum accreted icing mass on cylinder throughout the hindcast period (1957-2014).

Extreme/100 year values of accreted icing mass

The individual yearly maximum accreted icing mass at each grid point have been fitted to a Gumbel distribution to extract the 100 year extreme values (Figure 3). The maximum values are not increasing dramatically compared with Figure 2, from ~220 to ~240 tons (about 10%) in the north-eastern corner of the domain. The hindcast period already spans more than half a century, hence one should not expect that the 100 year values would be much higher. Some of the isolated maxima seen in Figure 2 are smoothed out and the north-east gradient in icing severity is becoming even more evident.

The dominant direction of ice accretion was determined by finding the compass direction of the panel on the cylinder with the highest extreme icing mass and the result is shown in Figure 4. The southern Barents Sea seems to be divided into three regions with respect to dominant direction of icing (Figure 4). In a region extending about 100 km from the coast, the dominant direction is from north-east, while in the central Barents Sea it is more directly from the north. East of 30°E, the direction again turns more to the north-east. For the grid points that are closest to shore, the direction is more variable and probably affected by cold winds blowing out from the mainland.

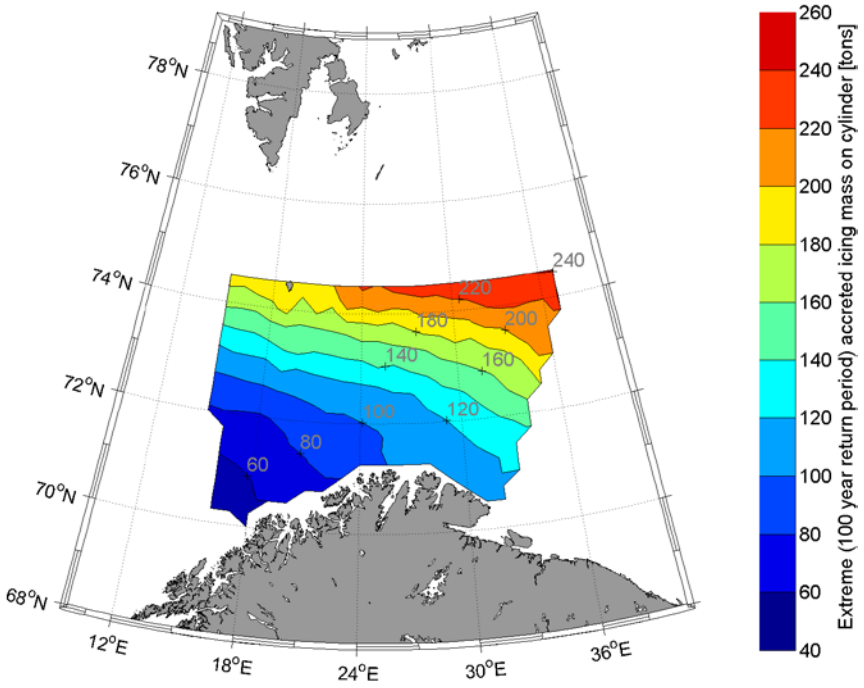

Figure 3 Extreme (100 year) accreted icing mass on cylinder.

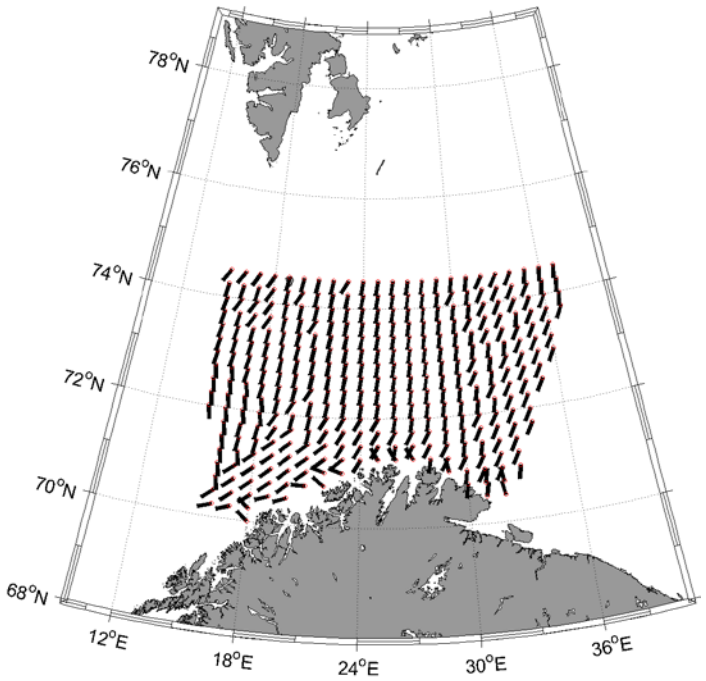

Figure 4 The dominant direction of the maximum ice accretion is plotted as arrows for each grid point. A red circle is drawn at the basis of each vector arrow.

Seasonal analysis

Monthly maxima of accreted icing mass throughout 1957-2014 are shown in Figure 5. The analysis reveals that there is very little icing from July to October. The most severe icing month is February. Interestingly, it takes some time for the east-west gradient in icing to build up when winter sets in, this is not fully established until January and could be related to when

sea ice starts forming in the north-eastern Barents Sea. The icing year appears to be a bit "asymmetrical", with more severe icing conditions in May than in December in the north-eastern corner of the domain.

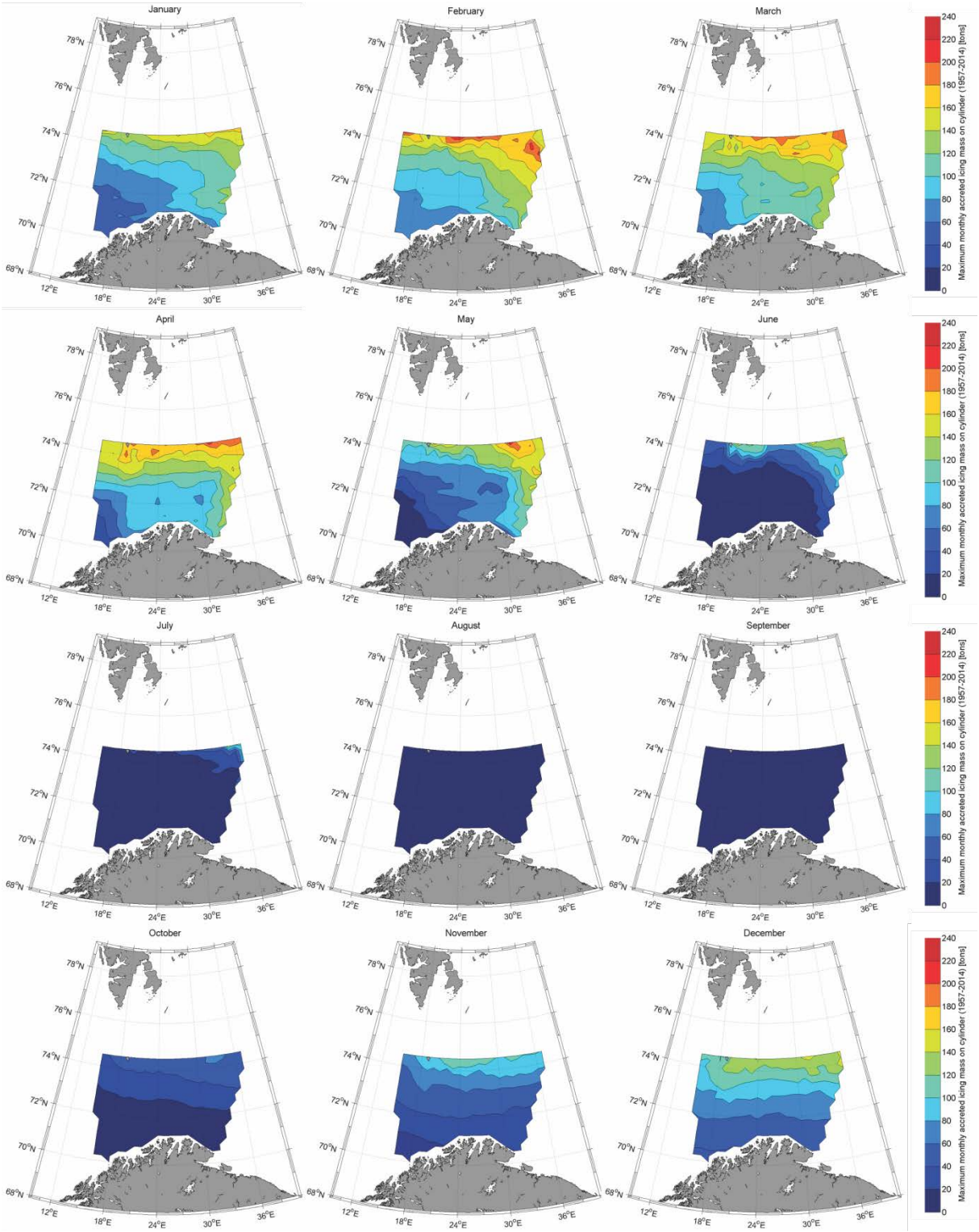

Figure 5 Monthly maximum accreted icing mass on cylinder throughout the hindcast period (1957-2014).

DISCUSSION

Convective heat loss to the air is an important factor in cooling sea spray below freezing to form icing, which combines both the effect of low temperature and high wind speeds. The convective heat loss Q_c [W/m^2] is given by

$$Q_c = h(T_b - T_a)$$

where T_b is the temperature of the brine on the icing surface, T_a is the air temperature, and h is the convective heat transfer coefficient. The brine temperature T_b is generally a time-dependent variable that depends on the freezing rate and salt capture of the icing process. For the purpose of comparing convective heat transfer at different locations in the Barents Sea, the freezing temperature of sea water T_f (assumed to be -1.8°C) is used instead, changing the expression to:

$$Q_c = h[(-1.8°\mathrm{C}) - T_a].$$

h depends on wind speed U_{10} [m/s^2] through the Reynolds number of the cylinder given by

$$Re_D = U_{10}D/\nu_a,$$

where ν_a is the kinematic viscosity of air. See (Hansen & Teigen, 2015) for the full expression used for the heat transfer coefficient for large cylinders. In Figure 6, the maximum convective heat loss calculated from the hindcast data is shown. A similar pattern as for the icing contour maps can be seen, with a north-east gradient. Maximum values of convective heat loss are about three times higher in the north-eastern corner of the domain than in the south-western corner, which is the same proportionality as for the estimates of total accreted icing mass (Figure 2). This indicates that convective heat loss could serve as a proxy for icing severity.

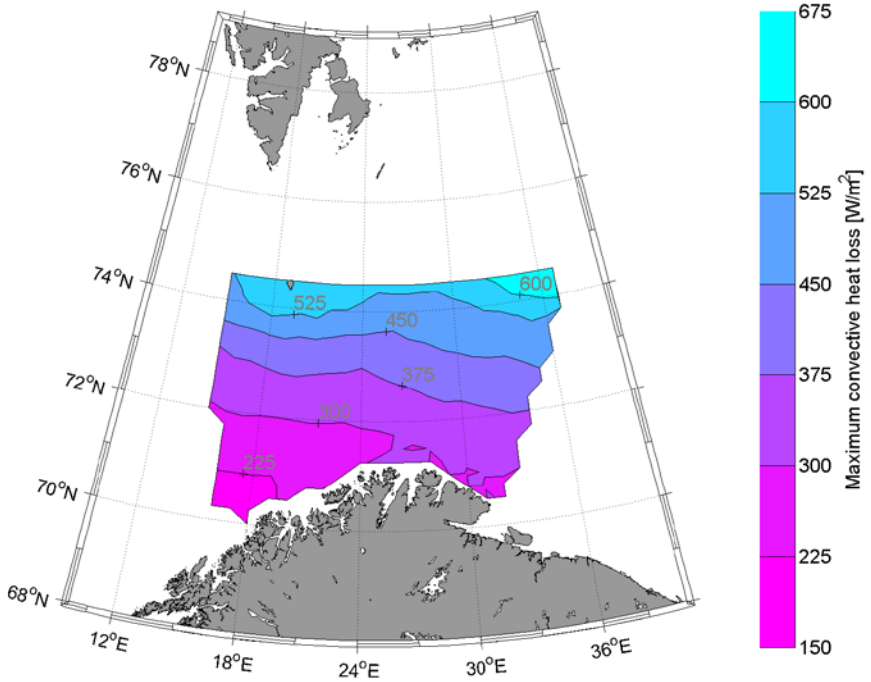

Figure 6 Maximum convective heat loss (1957-2014) from brine layer on the surface of the reference cylinder.

The north-east gradient in extreme icing mass and heat loss reflects the decrease in air temperature as one moves north and east in the Barents Sea. In south-west, warm Atlantic water masses are entering the Barents Sea, moderating the winter air temperatures and keeping the southern Barents Sea ice-free. Closer to the ice edge in the north-east, outbreaks of cold air from the north are more common. The presence of sea ice in the Barents Sea has a profound effect on the air temperature and a correlation analysis could reveal the influence of the distance from the ice edge on the icing severity at a given location.

A regional analysis of icing severity is useful for several purposes. It shows that there is quite considerable variation within the Barents Sea and challenges the use of a uniform icing profile north of 68^{o}N in the NORSOK N-003 standard (NORSOK, 2007). It gives a quick indication of the seasonal variation in icing severity and promotes an early recognition of the potential icing issues for new oil and gas developments in the area. For more detailed analyses, there is a need for more field observations of sea spray formation and icing from relevant vessels and structures to calibrate and reduce the uncertainty in the underlying numerical models.

SUMMARY

Basin-wide estimates of marine icing in the Barents Sea have been made for the entire hindcast period (1957-2014). The simulations reveal the spatial and temporal structure of the severity of marine icing and the worst directions for ice build-up. This kind of regional analysis enables a quick upfront evaluation of the icing severity in the early phases of an oil and gas project.

REFERENCES

Boards of inquiry and disciplinary courts, 1942. *Board of Inquiry into loss of HM Whalers SHERA and SULLA: recommendations on icing problems in Russian waters,* Kew, England: The National Archives.

Edwards, B., 2002. *The Road to Russia: Arctic Convoys 1942.* 1st red. s.l.:Pen & Sword Books Ltd.

Hansen, E. S., Eik, K. J. & Teigen, S. H., 2015. *Statistical methods for applying icing estimates in offshore design.* Trondheim, International Conference on Port and Ocean Engineering under Arctic Conditions (POAC).

Hansen, E. S. & Teigen, S. H., 2015. *An efficient numerical model for marine icing.* Trondheim, International Conference on Port and Ocean Engineering under Arctic Conditions (POAC).

Jørgensen, T. S., 1984. *Sjøsprøytmålinger på boreriggen "Treasure Scout" - Resultater fra forsøk april 1983 - februar 1984,* Trondheim, Norway: Norges Hydrodynamiske Laboratorier.

National Oceanographic Data Center, 2013. *World Ocean Atlas 2013,* s.l.: s.n.

NORSOK, 2007. *N-003 Action and action effects, ed. 2,* Oslo, Norway: Standards Norway.

Reistad, M., 2010. A high-resolution hindcast of wind and waves for the North Sea, the Norwegian Sea, and the Barents Sea. *Journal of Geophysical Research.*

Reistad, M., 2011. A high-resolution hindcast of wind and waves for the North Sea, the Norwegian Sea, and the Barents Sea. *Journal of Geophysical Research,* 116(C5).